

学位論文（要約）

**Development of an in-situ K-Ar isochron dating method
for landers on the Moon and Mars**

（月・火星着陸機用）

その場 K-Ar アイソクロン年代計測法の開発）

平成 25 年 12 月 博士（理学）申請

東京大学大学院理学系研究科

地球惑星科学専攻

長 勇一郎

This Dissertation is dedicated to
Fumiko Cho,
who passed away on October 21, 2013, at the age of 89,
and
Jiro Oizumi,
who passed away on June 28, 2012, at the age of 26.

Acknowledgments

I express my deep gratitude to Professor Seiji Sugita, my research supervisor, for his patient guidance, enthusiastic encouragement and useful critiques of my research work.

I would like to express my very great appreciation to Dr. Yayoi N. Miura for every support and instruction about designing the instruments and actual experiments as well as interpreting the results. This work would not have been possible without her contributions.

This research effort was greatly enhanced by Dr. Tomokatsu Morota, Nagoya University, who provided constructive inputs for crater chronology and the application of in-situ analyses using my instrument. This research was greatly benefitted from the critical comments by Prof. Hiroko Nagahara. Constructive and critical comments by Dr. Yasuhito Sekine, Univ. Tokyo, are also gratefully acknowledged. I am thankful to Dr. Ryuji Okazaki of Kyushu University for forming the foundation of this research.

I appreciate invaluable suggestions and advices about noble gas analyses by Prof. Keisuke Nagao. He also generously provided the mineral samples used in this research. I also thank the discussions with Prof. Tetsumaru Itaya of Okayama University of Science. This work was benefitted from many helpful suggestions and technical supports about noble gas analysis from Prof. Takafumi Hirata of Kyoto University, Dr. Hirochika Sumino of Univ. Tokyo, Prof. Ichiro Kaneoka, and Dr. Ken-ichi Bajo of Hokkaido University.

This work benefitted from the discussions about Mars with Prof. Hideaki Miyamoto, and Dr. Goro Komatsu and Dr. Tomohiro Usui. I would like to thank Prof. Masaki Ogawa, Univ Tokyo, for the insightful discussions concerning the thermal evolution of the planets.

I thank Dr. Ko Ishibashi and Dr. Sosuke Ohno for experimental supports and extensive suggestions on LIBS measurements. Dr. Shun-ichi Kamata is gratefully acknowledged for sample preparations and XRF measurements as well as the discussions to improve my research. Dr. Tomoko Arai generously supplied the powdered rock samples used for LIBS calibration. I am grateful to Prof. T. Yagi of Ehime University and Dr. H. Goto of the University of Tokyo for helping us to make the pellet samples with a high-pressure cubic press at Institute of Solid State

Physics, the University of Tokyo. The gneiss samples were provided by Dr. Naoyoshi Iwata of Yamagata University. I thank Dr. Kenji Mibe at the Earthquake Research Institute for preparing for the basaltic glass sample containing Ar. Prof. Tsuyoshi Komiya of Univ. Tokyo generously supplied natural rock samples collected from Greenland. Prof. Kazuhito Ozawa kindly provided basaltic rock samples for laser ablation experiments. I would like to thank both technical and scientific supports provided by Dr. Tatsu Kuwatani and Mr. Hideto Yoshida for ion microprobe analysis. Mr. Takashi Sakai and Ms. Megumi Mori are gratefully acknowledged for preparing the samples for EPMA analysis.

Dr. Jun-ichi Haruyama and Dr. Makiko Ohtake are acknowledged for their instructions and discussions about the lunar surface. This study greatly benefitted from the helpful discussions about lunar samples with Dr. Yuzuru Karouji, Dr. Hiroshi Nagaoka, and Prof. Hiroshi Takeda. Discussions with Dr. Risa Sakai is gratefully acknowledged.

I appreciate the discussion with the members of the Japanese decadal survey: Prof. Noriyuki Namiki, Prof. Satoshi Tanaka, Prof. Toshifumi Mukai, and Dr. Kazunori Ogawa. Discussions with Dr. Shingo Kameda and his students at Rikkyo University are also gratefully acknowledged.

I wish to thank Dr. Barbara A. Cohen of Marshall Space Flight Center, for many discussions and continuous encouragements.

Expert technical help by Mr. Atsushi Saito of the workshop, Univ. Tokyo, Mr. Hideki Saitou (Fuji imvac), Mr. Satoshi Miyata (NIC Autotec), Mr. Mitsuru Onobe (Toyoko chemistry), Mr. Noboru Yamamoto (Osaka Vacuum), Mr. Kunihiro Aoshima (Adcap Vacuum), and Mr. Rin Yamamoto (R Vacuum Laboratory) was essential for the construction of the laser ablation system. I greatly thank Mr. Shigemi Oki (Keyence) for the loan of microscopes.

Supports from Mrs. Yumi Hirata and Mrs. Yoko Ohuchi are gratefully acknowledged. I thank the assistance and advices by lab members.

I appreciate the financial support of the JSPS Research Fellow. This work was supported in part by a research fund by ISAS/JAXA.

Finally, I express my deepest gratitude to Professor Takafumi Matsui for his introduction to this research field and continuous encouragements.

Abstract

Age is one of the most important factors for the interpretation of the geologic record. The ages of most planetary surfaces have been estimated with crater counting (i.e., crater chronology) based on image data. The crater chronology model has been calibrated with the radiometric ages of the Apollo samples. However, no calibration samples have been obtained for the lunar surfaces before 4 Ga (billion years ago) or between 3.0-0.1 Ga. The lack of such data led many authors to propose different models, such as Late Heavy Bombardment model [Stöffler and Ryder, 2001], the continuous decay model [Neukum, 1983], and the decreasing flux model [Hartmann *et al.*, 2007]. Furthermore, the Martian absolute ages may have uncertainties of about a factor of 2-4 because of the lack of directly dated samples with clear locality information [Hartmann and Neukum, 2001].

Thus, many sample-return missions have been proposed in the last several decades. However, no sample-return mission has occurred from planets or satellites (e.g., the Moon or Mars) since Apollo because of its high cost and technical difficulties. Consequently, in-situ dating planetary mission without sample return is very important. In addition to the lower cost, in-situ dating is valuable because of the ability of iterative and multiple measurements while traversing the planetary surfaces. In fact, several in-situ geochronology techniques have been developed or proposed for the missions including the British Beagle 2 lander and the NASA's Curiosity rover. Most recently, Curiosity conducted the first in-situ dating experiments on Martian rock and obtained 4.21 ± 0.35 Ga for a mudstone on the floor of Gale crater [Farley *et al.*, 2013]. However, the noble-gas analyses of shergottites revealed significant excess ^{40}Ar derived from the Martian mantle, which would cause a large error for the whole-rock analyses proposed by the previous missions including Curiosity. In order to solve these problems, isochron measurements are essential.

This study proposes a new in-situ geochronology method that can analyze individual crystals locally using laser ablation technique, in order to construct a K-Ar isochron plot from a single rock sample. We use laser-induced breakdown spectroscopy (LIBS) and quadrupole mass spectrometer (QMS) for the measurements of K and Ar, respectively. The purpose of this thesis research is to develop and demonstrate this method by establishing individual key techniques, such as (i) accurate

and precise K measurement, (ii) quantitative Ar measurements from a small laser ablation spot, and (iii) acquisitions of actual K-Ar isochron ages using a combination of flight-proven instruments.

First, we developed K measurements using LIBS. A LIBS measurement had to be carried out under a high vacuum condition necessary for mass spectrometry of a trace amount of Ar gas. One of the largest challenges for the LIBS-QMS approach is to measure K accurately and precisely because the emission of laser-induced plasma is generally very weak under high vacuum conditions [*Knight et al.*, 2000]. Although a previous study reported the results of quantitative measurements of K under atmospheric pressure [*Stipe et al.*, 2012], no study has been able to measure the concentration of K under high vacuum conditions with acceptable precisions. We constructed a sensitive detection system specific for K emission lines and used an internal normalization approach to measure K emission accurately. We obtained a precise calibration curve that can determine the K abundance down to the detection limit of $K_2O=300$ ppm and quantitation limit of 1000 ppm. We also evaluate the precision achievable with our approach. The precision would be 20% for a rock containing 1 wt% of K, but we suggest K-Ar age would be measurable with an acceptable precision (better than 20%) by considering the error propagation.

Second, we conducted age determination experiments with the LIBS-QMS approach based on the K calibration model we developed. We combined K measurements with Ar measurements coupled with volume measurements of laser-ablation cavities to determine the K-Ar ages for geologic samples. In order to validate this method, we measured the K-Ar model ages of the homogeneous pellet samples made of pristine minerals with known ages and K content. The validation results suggest that the LIBS-QMS approach can measure the K-Ar ages with an accuracy of better than 25% and a precision of 20% except for highly brittle materials, such as the plagioclase pellet used in this study. Spallation from laser ablation cavity on these samples prohibits an accurate age measurement because the true cavity volume cannot be measured accurately. This observation suggests the mechanical strength of the sample is important for K-Ar dating using this method.

Next, we measured a couple of gneiss slabs to verify the capability of isochron measurements for natural rocks. When we construct a K-Ar isochron (i.e., $^{40}Ar/^{36}Ar$ vs. $^{40}K/^{36}Ar$), the data points follow a straight line well, strongly suggesting the feasibility of isochron measurements with our LIBS-QMS approach. One sample yielded an isochron age of 640 ± 120 Ma, which is systematically larger than the known value by ~30% but consistent with the reported K-Ar ages within 2-sigma

error. From the intercept of the isochron, we obtained the initial Ar isotopic ratio $^{40}\text{Ar}/^{36}\text{Ar}$ of 480 ± 130 , which is comparable to that of atmospheric contamination ($^{40}\text{Ar}/^{36}\text{Ar}=296$). These results strongly suggest that the isotopic composition of trapped Ar is measurable with this approach. This ability would provide insights into the evolution of the parent magma.

The other sample did not contain much ^{36}Ar derived from the terrestrial atmosphere; the amount of ^{36}Ar was not significantly larger than the blank level. Thus, we drew the ^{40}Ar - ^{40}K plots based on the concentrations of ^{40}K and ^{40}Ar , after checking the most of ^{40}Ar is radiogenic in origin. The “isochron” slopes yielded 500 ± 160 Ma for the 485 ± 35 Ma sample and 1230 ± 250 Ma for the 1050 ± 10 Ma sample, suggesting the validity of this approach. The intercept of ^{40}Ar - ^{40}K plot yielded the trapped ^{40}Ar of $\sim 10^{-6}$ cm³ STP/g, which is consistent with the amount of excess ^{40}Ar contained in the shergottites [Bogard *et al.*, 2009]. The LIBS-QMS analyses yield variable K concentrations, which is difficult to achieve with whole-rock analyses proposed in previous studies. We also found the LIBS-QMS measurements yield averaged compositions for the minerals in an ablation spot. This property suggests that a wide range of K concentrations and thus a reliable isochron can be obtained even though the variety of K-bearing phases is limited. We also identified the factors that potentially cause scattering in isochron diagram and proposed several criteria to obtain reliable isochrons: the spallation of the laser-ablation cavity, the variation of K concentrations within an ablation spot, and the contribution of blank gases to ^{36}Ar signal.

The above experimental results using test samples do not guarantee the applicability of our LIBS-QMS isochron method for actual rock samples on planetary surfaces. Depending on geologic units, the types of rocks and K concentration vary greatly on planetary surfaces. Thus, we assess the capability of our in-situ K-Ar dating method taking the petrologic properties including K abundance and possible age range of the Moon and Mars surfaces into account. First, we examined the global maps of K obtained with the Gamma Ray Spectrometers onboard remote sensing satellites and found the concentrations of K and Ar of KREEPy materials are well above the detection limits of our LIBS-QMS method. Then, the elemental compositions and textures of KREEP basalt were investigated. We found that Si-rich glasses contained in mesostasis are measurable with K-Ar dating on the Moon because of the high K concentration (~ 7 wt%) while other minerals (i.e., pyroxene, olivine, and plagioclase) contain virtually no K. Since the textures of these samples were heterogeneous at the scale of laser spot (~ 500 μm), the “isochron” ages would be obtained by

measuring the different portions containing K-bearing phases in various ratios. The major problem concerning in-situ K-Ar dating is partial ^{40}Ar loss due to thermal events after crystallization. This suggests that K-Ar dating only yields the lower limit for the real crystallization age. Furthermore, brecciation by impacts and contamination by solar wind will inhibit accurate in-situ dating. In order to avoid such problems and obtain meaningful age data by in-situ dating, we need to find fresh samples on planetary surfaces. Although very large drills or ablator tools would be able to solve this problem by artificially exposing fresh surfaces of rocks, finding outcrops where many rock samples have naturally exposed fresh surfaces would be better in terms of reducing cost and technical difficulty of mission plan. Thus, we searched for such outcrops on the Moon and Mars. In particular, we conduct a detailed case study with Aristillus crater, which is located at the Procellarum KREEP Terrane on the Moon in this study. On the basis of high-resolution images on the impact melt sheet of Aristillus crater, we propose that measuring fresh boulders excavated by a recent small impact (crater diameter ~ 100 m) is effective for correlating the age of a rock sample to a geologic unit and for avoiding the problems such as the contamination by the solar wind, the reset of the K-Ar age and later brecciations by impacts.

Finally, we evaluated how our method can constrain the absolute chronology models of the Moon and Mars based on the precisions of age measurements achieved by this study. Assuming the K concentration found by the landing missions on Mars and cratering model ages, our method is estimated to be able to determine the age of Hesperian-Amazonian boundary with 10-15% precision and constrain the duration of volcanic activities, the timing of outflow channels formation, and the absolute age when cold and dry climate started prevailing the planet. Furthermore, the absolute age of impact melt rocks in Aristillus crater, whose ages correspond to the “missing ages” of the current lunar crater chronology model (i.e., between 3.0 Ga and 0.1 Ga), would be measured with $\sim 20\%$ precision when the K concentration of the glass in KREEP basalt is assumed. Then, our method would be able to discriminate the constant flux model [Neukum, 1983] and the decreasing flux model [Hartmann *et al.*, 2007]. The implications of in-situ dating in Aristillus crater include refining the crater chronology model, determining the age of the youngest mare basalts, which provides insights into the origin of the Moon, and understanding the dynamical evolution of the asteroids in the last three billion years.

Contents

Acknowledgments	iii
Abstract	v
Contents	ix
List of Figures.....	xi
List of Tables	xiv
Chapter 1 General Introduction	15
1. Surface chronology on the Moon and Mars	16
1.1. Crater chronology	16
1.2. Uncertainties in chronology models	21
2. Need for in-situ dating and approaches by previous studies	25
3. Objectives of this study	27
4. Outline of this dissertation	28
Chapter 2 Quantitative potassium measurements using laser-induced breakdown spectroscopy under high vacuum conditions for in-situ K-Ar dating of planetary surfaces.....	30
Abstract	31
1. Introduction	31
2. Experimental	36
2.1 Measurement system	36
2.2 Calibration samples	37
2.3 Spectral analysis	39
3. Results & Discussion	41
3.1 LIBS spectra	41
3.2 Calibration curve	45
3.3 Prediction band and calibration error	47
3.4 Capability to measure rocks on planetary surfaces	49
4. Conclusions	49

Chapter 3	An in-situ K-Ar isochron dating method for planetary landers using laser-ablation technique.....	51
Abstract		52
1	Introduction	54
2	Experiments and methods	55
2.1	K-Ar dating	55
2.2	Concept of LIBS-QMS approach	58
2.3	Measurement procedure	61
2.4	Samples	62
3	K-Ar age determination	67
3.1	Model ages of the mineral samples	67
3.2	K-Ar isochron for natural rock samples	75
3.3	Age determination error	88
4	Conclusions	91
Chapter 4	Feasibility of in-situ K-Ar dating on the Moon and Mars .	93
Abstract		94
1.	Introduction	95
2.	Capability of measurements of K and Ar	96
2.1	Lunar samples	96
2.2	Martian samples	105
3.	A case study for K-Ar dating on the Moon: strategies for meaningful age measurements	113
4.	Constraining chronology models and its implications for lunar and Martian evolution	118
5.	Future developments	123
6.	Conclusions	124
Summary	126
Appendices	130
A	Experimental apparatuses	131
B	Time interpolation of QMS signals	134
C	Sensitivity calibration of quadrupole mass spectrometer	135
D	Variation of blank level	137
E	Elemental maps of gneiss samples	138
References	140

List of Figures

Figure 1.1 Crater size-frequency distribution (CSFD) for three geologic units in Mare Orientale on the Moon	18
Figure 1.2 Spatial distribution of the crater retention ages of mare basalts on the lunar surface	18
Figure 1.3 Martian crater chronology model	19
Figure 1.4 Spatial distribution of major geologic units on Mars	21
Figure 1.5 Comparison of various crater chronology models for the Moon	24
Figure 1.6 Comparison between (a) an isochron analysis and (b) a whole-rock analysis	27
Figure 2.1 (Upper) Shape of laser-induced plasma for a variety of ambient pressures. (Lower) Emission intensities of Si and Mg lines as a function of ambient pressure	34
Figure 2.2 Schematic diagram of the experimental setup	36
Figure 2.3 High-resolution spectra for xenolith and nephelinite samples around the K emission lines	40
Figure 2.4 Emission spectra of five standard samples under the vacuum condition	41
Figure 2.5 Close up of the spectrum for JR-1 and the peaks fitted with five Voigt functions	42
Figure 2.6 Potassium line intensity (a) and intensity ratio I_K/I_O (b) as a function of pulse number	44
Figure 2.7 Calibration curve for K_2O	46
Figure 2.8 Percent uncertainties computed from the prediction band for 95% and 68% confidence levels.	48
Figure 2.9 Known vs. predicted potassium concentrations.	48
Figure 3.1 Schematic diagram of the LIBS-QMS system	60
Figure 3.2 Photograph of the experimental system	64
Figure 3.5 Potassium map of (a) pyroxene gneiss and (b) hornblende biotite gneiss	65
Figure 3.6. (a) Comparison of LIBS spectra for biotite ($K_2O=8.46$ wt%), plagioclase ($K_2O=1.42$ wt%), and hornblende pellets ($K_2O=1.12$ wt%). (b) Spectra around K emission lines at 764.4 nm and 769.9 nm	68
Figure 3.7 Mass spectra of the gases released from the hornblende, biotite, and plagioclase pellet samples	71
Figure 3.8. Cross sections of laser-ablation craters on the mineral pellet samples	71
Figure 3.9 Emission and mass spectra for the two different spots (spot #9 in red, spot #14 in blue) of the hornblende-biotite bearing gneiss.	76

Figure 3.10 Potassium-Argon isochron for a hornblende-biotite gneiss sample	78
Figure 3.11 Variation in K signal as a function of laser pulse number	81
Figure 3.12 Emission spectra of laser-induced plasma for the 1st, the 400th, and the 1000th laser shots.....	81
Figure 3.13 Comparison between laser-ablation cavities	82
Figure 3.14 K-Ar isochron plot using the all data for the hornblende-biotite gneiss	83
Figure 3.15 ^{40}Ar - ^{40}K plot for (upper) hornblende-biotite gneiss and (lower) pyroxene gneiss samples	86
Figure 3.16 Precision of K-Ar age calculated by error propagation.....	89
Figure 3.17 Precision of age determination as a function of K and Ar contents	90
Figure 4.1 Global map of K on the Moon obtained by Kaguya gamma ray spectrometer	97
Figure 4.2 Photograph of a thin section of KREEP basalt 15382.....	99
Figure 4.3 Sketch of a thin section of the KREEP basalt 15382	99
Figure 4.4 Sketch of another region of sample 15382	100
Figure 4.5 Photograph of a thin section of KREEP basalt 15386.....	100
Figure 4.6 Ar release pattern for the whole rock of 15382.....	101
Figure 4.7 Precision of our in-situ K-Ar dating method for different conditions of lunar geologic units	104
Figure 4.8 Global map of K on Mars obtained by gamma ray spectrometer onboard Mars Odyssey	106
Figure 4.9 Thin sections of Shergotty.....	107
Figure 4.10 Back-scattered electron image of Yamato 980459.....	108
Figure 4.11 Mineral map for two Zagami thin sections.....	108
Figure 4.12 Ar release diagram for Shergotty meteorite	109
Figure 4.13 Texture of NWA 817 nakhlite.....	109
Figure 4.14. Precision of our in-situ K-Ar dating method for different conditions of Martian geologic units	112
Figure 4.15 (A) Aristillus crater on the Moon. (B) Schematic drawing of the cross section of Aristillus crater. (C) Small crater on the Aristillus crater floor with the boulders ejected by the crater-forming impact.....	114
Figure 4.16 Schematic diagram showing the age measurements of multiple rocks in Aristillus crater	117
Figure 4.17 Possible Martian history corresponding to the different chronology models.....	121
Figure 4.18 Possible age determination results for Aristillus crater for different chronology models	122
Figure 6.1 Experimental system	131
Figure 6.2 Optical system for focusing laser pulses and monitoring the surface of samples	132
Figure 6.3 Light collecting optics and the viewing geometry	132
Figure 6.4 Field of view (FOV) of the spectroscopic observations.....	133

Figure 6.5 Sample holder and a pellet sample	133
Figure 6.6 Schematic diagram of time interpolation used for correcting the differences in the timing of individual mass peak measurements	134
Figure 6.7 Schematic diagram of the calibration line	135
Figure 6.8 Time variation of QMS signals of ⁴⁰ Ar with the different SEM voltages	136
Figure 6.9 Sensitivity of the QMS system in terms of ⁴⁰ Ar for different SEM voltages used in this study	137
Figure 6.10 Stability of blank levels for the mass number of 36, 38, and 40	137
Figure 6.11 Elemental map of pyroxene-bearing gneiss.	138
Figure 6.12 Elemental map of hornblende-biotite-bearing gneiss.	139

List of Tables

Table 2.1 Potassium concentrations of the calibration standards used in this study	38
Table 3.1 Concentrations of K in the minerals of the gneiss samples.	66
Table 3.2 Summary of analyses for three mineral samples	74
Table 3.3 Summary of isochron data for the hornblende biotite gneiss and pyroxene gneiss.....	87
Table 4.1 Characteristics of high-K craters and their cratering model ages	114

Chapter 1

General Introduction

本章については、五年以内に雑誌等で刊行予定のため、非公開。

Chapter 2

Quantitative potassium measurements using laser-induced breakdown spectroscopy under high vacuum conditions for in-situ K-Ar dating of planetary surfaces

This chapter is to be submitted to *Spectrochimica Acta Part B*, written by

Cho, Y., S. Sugita, K. Ishibashi, S. Ohno, S. Kamata, T. Arai, Y. N. Miura, T. Morota, N.
Namiki and T. Matsui

本章については、五年以内に雑誌等で刊行予定のため、非公開。

Chapter 3

An in-situ K-Ar isochron dating method for planetary landers using laser-ablation technique

This chapter is to be submitted to *Journal of Geophysical Research, Planets*, written by Cho, Y., S. Sugita, Y. N. Miura, R. Okazaki, and T. Morota.

本章については、五年以内に雑誌等で刊行予定のため、非公開。

Chapter 4

Feasibility of in-situ K-Ar dating on the Moon and Mars

本章については、五年以内に雑誌等で刊行予定のため、非公開。

Summary

A new in-situ K-Ar isochron dating method was developed in this dissertation work. We used the laser ablation technique and constructed actual system both emission spectroscopy and noble gas analysis using the combination of the flight-proven instruments.

In Chapter 2, we developed the method to quantitatively measure the concentration of K using laser-induced breakdown spectroscopy (LIBS). One of the largest challenges for the LIBS-QMS approach lied in measuring K accurately and precisely because the emission of laser-induced plasma is significantly decreased under high vacuum conditions. We constructed a sensitive detection system specific for the K emission lines and used an internal normalization approach to obtain K emission accurately. We obtained a precise calibration curve and determine the detection limit of 300 ppm and quantitation limit of 1000 ppm. We also evaluate the precision achievable with our approach. The precision would be 20% for a rock containing 1 wt% of K, but we suggest K-Ar age would be measurable with an acceptable precision (better than 20%) by considering the error propagation.

In Chapter 3, the main part of this dissertation, deals with the results of age determination with our LIBS-QMS approach. Experimental setup and results are illustrated in detail. We combine K measurements with Ar measurements coupled with volume measurements of laser-ablation cavities to determine the K-Ar ages for geologic samples. In order to verify this method, we derive the K-Ar model ages of the mineral samples with known ages and K content. The results suggest that the LIBS-QMS approach can measure the K-Ar ages with an accuracy of better than 25% and a precision of 20% except for brittle materials, from which we found that the spallation of laser ablation cavity prohibit an accurate age measurement because we would never know the real volume of the cavity. This observation suggests the mechanical strength of the sample is important for K-Ar dating using this method.

Next, we measured a couple of gneiss slabs to verify the capability of isochron measurements for natural rocks. When we construct a K-Ar isochron (i.e., $^{40}\text{Ar}/^{36}\text{Ar}$ as a function of $^{40}\text{K}/^{36}\text{Ar}$), the data points aligned well along a straight line, strongly suggesting the feasibility of isochron measurements with our LIBS-QMS approach. One sample yielded an isochron age of 640 ± 120 Ma, which is consistent with the reported K-Ar ages within the 2-sigma error. From the intercept of the isochron, we obtained the initial Ar isotopic ratio $^{40}\text{Ar}/^{36}\text{Ar}$ of 480 ± 130 , which is comparable to that of atmospheric contamination ($^{40}\text{Ar}/^{36}\text{Ar}=296$). Because the other sample did not contain much ^{36}Ar

derived from terrestrial atmosphere, the amount of ^{36}Ar was not significantly larger than the blank level. Thus, we drew the ^{40}Ar - ^{40}K plots based on the concentrations of ^{40}K and ^{40}Ar , after checking the most of ^{40}Ar is radiogenic in origin. The “isochron” slopes yielded 500 ± 160 Ma for the 485 ± 35 Ma sample and 1230 ± 250 Ma for the 1050 ± 10 Ma sample, suggesting the validity of this approach. The intercept of ^{40}Ar - ^{40}K plot yielded the trapped ^{40}Ar of $\sim 10^{-6}$ cm³ STP/g, which is consistent with the amount of excess ^{40}Ar contained in the shergottites [Bogard *et al.*, 2009]. Thus, we concluded that our LIBS-QMS method is capable of measuring K-Ar ages locally and deriving the contribution of initially trapped ^{40}Ar based on isochron measurements, in contrast to the approaches previously proposed. We also identified the factors that potentially cause scattering in isochron diagram and proposed several criteria to obtain reliable isochrons: the spallation of the laser-ablation cavity, the variation of K concentrations within an ablation spot, and the contribution of blank gases at 36 amu.

In Chapter 4, we assess the feasibility of the in-situ K-Ar dating we develop in this dissertation based on the data from meteorites, returned samples and remote-sensing missions of the Moon and Mars. Finding an appropriate sample is critical for in-situ age determination. First, we examined the global K maps obtained with the Gamma Ray Spectrometers onboard remote sensing satellites and found the concentrations of K and Ar of KREEPy materials are well above our detection limits of the LIBS-QMS method. Then, the elemental compositions and textures of KREEP basalt were investigated. We found that Si-rich glasses resident in mesostasis are suitable for K-Ar dating on the Moon because of the high K concentration (~ 7 wt%). The major problem is that partial ^{40}Ar loss due to subsequent thermal events found in Ar release pattern would only yield the lower limit for the real crystallization age. In order to avoid such problems and obtain meaningful age data by in-situ dating, we conduct a case study with the Aristillus crater, located at the nearside of the Moon. On the basis of high-resolution images on the impact melt sheet of Aristillus crater, we propose that measuring fresh boulders excavated by a recent small impact (crater diameter ~ 100 m) is effective for relating a rock sample to a geologic unit and for avoiding the problems such as the contamination by the solar wind, the reset of the K-Ar age and later brecciation by impacts.

Finally, we summarize the dissertation and discuss how our method can constrain the chronology of planets. We concluded that our method would be able to determine the age of the Hesperian-Amazonian boundary with 10-15% precision and provides implication for the duration of volcanic activities as well as outflow channel formation (Figure 4.17). Furthermore, by measuring

the absolute age of impact melt rock in Aristillus crater corresponding the “missing ages” of current lunar chronology (i.e., between 3.0 Ga-0.1 Ga), our method would be able to discriminate the constant flux model and decreasing flux model (Figure 4.18). The implication of such measurements would include the improvement of crater chronology model, the timing of youngest mare basalt on the Moon and the insight into the origin of the Moon, and the dynamical evolution of asteroids.

Appendices

A Experimental apparatuses

The photographs of actual instrument and detailed experimental setups are shown in this section.

The construction of the system is described in detail in *Cho 2011, Master Thesis*.

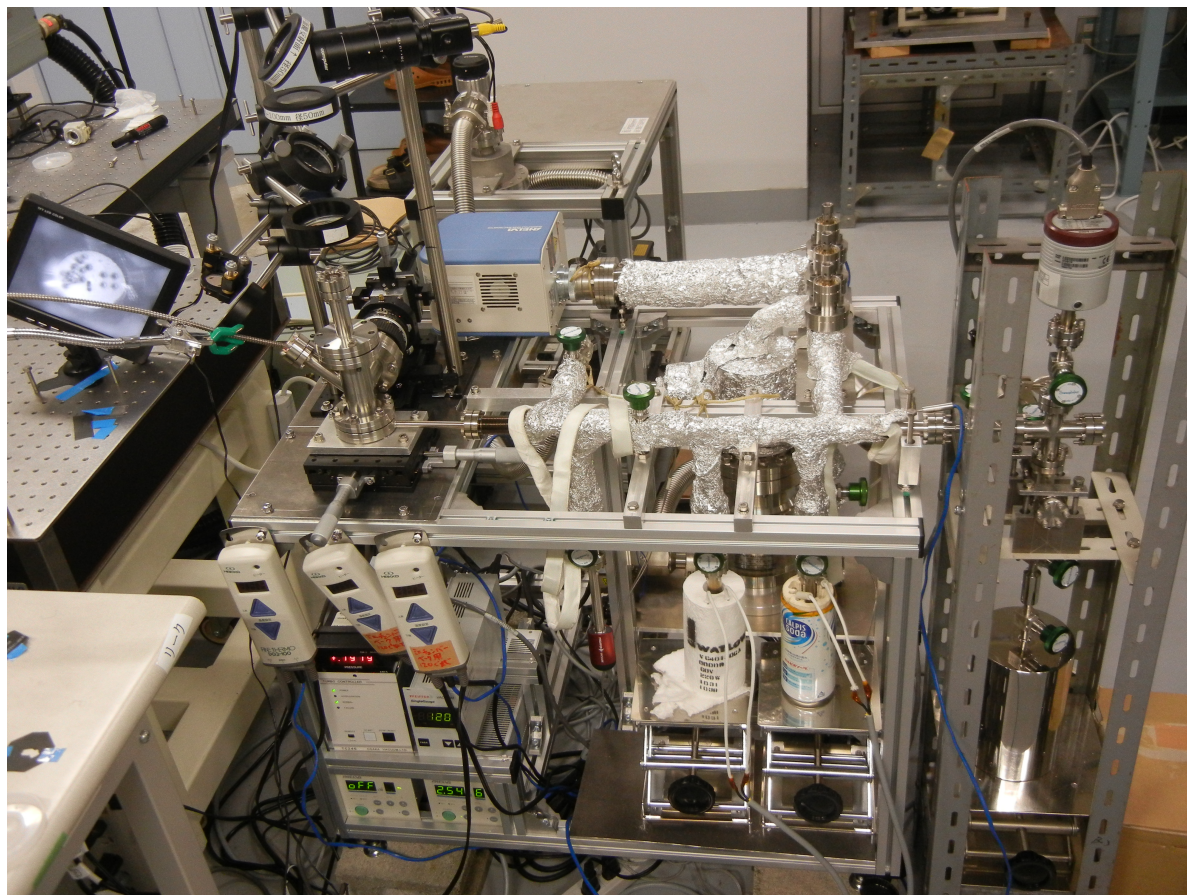


Figure 6.1 Experimental system. The width of the frame is approximately 75 cm. An auxiliary vacuum line equipped with a calibration gas tank is connected with the QMS system but is isolated except for the calibration of QMS. The function of each component is described in Chapter 3 with a schematic diagram (Figure 3.1).

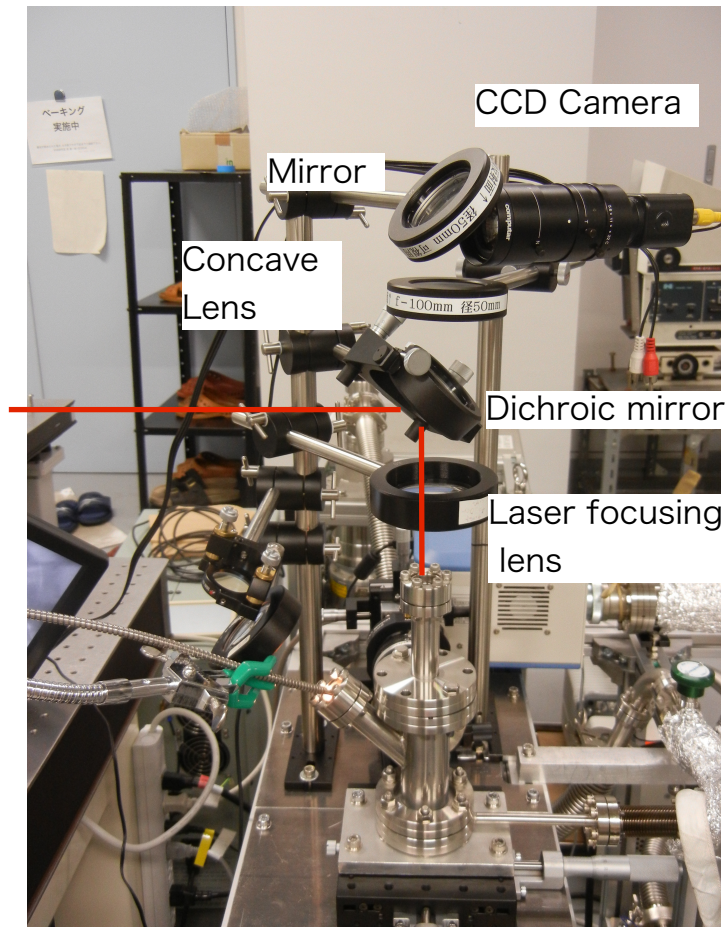


Figure 6.2 Optical system for focusing laser pulses and monitoring the surface of samples with a CCD camera.

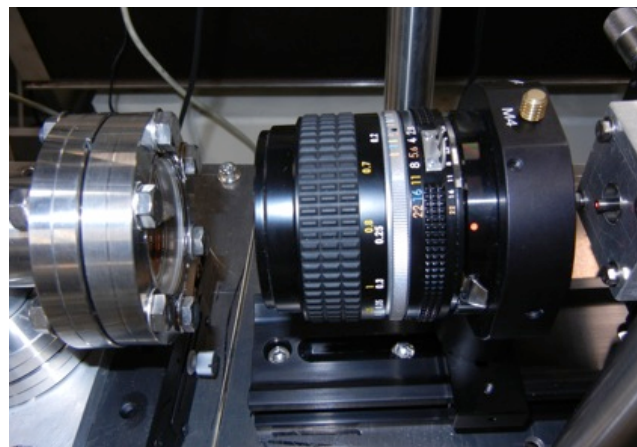


Figure 6.3 Light collecting optics and the viewing geometry. The focusing lens is placed at the side of the viewing window of the chamber. The emission from plasma is collected by the lens and focused onto the core of an optical fiber.

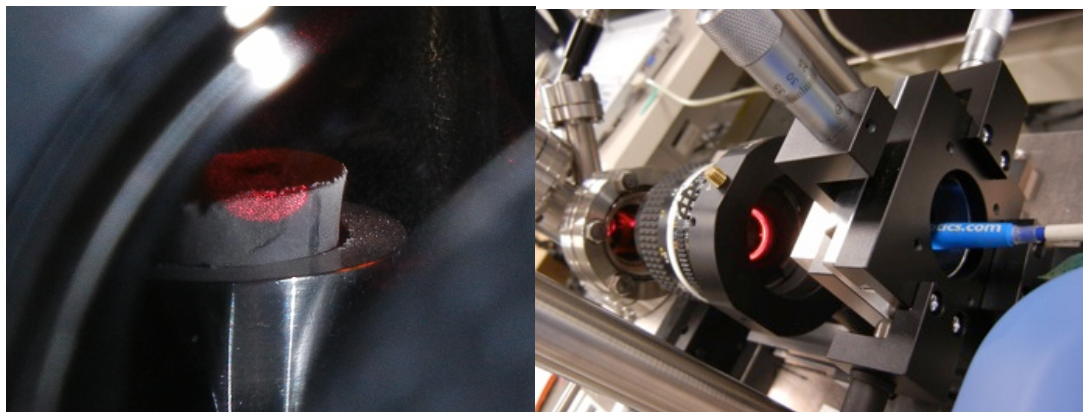


Figure 6.4 Field of view (FOV) of the spectroscopic observations. The size of FOV of the spectrometer was estimated to be ~ 8 mm in diameter by introducing the light from the other side of the optical fiber.



Figure 6.5 Sample holder and a pellet sample. The vertical position of the sample surface is adjustable. Each part is made of the stainless steel. For a scale, the diameter of the pellet sample is ~ 10 mm.

B Time interpolation of QMS signals

In general, the peak signals of QMS exhibit temporal variation during a measurement process. In order to determine the isotopic compositions and abundances of Ar accurately, we define the signal intensities by time interpolation and a regression analysis to the time of gas introduction.

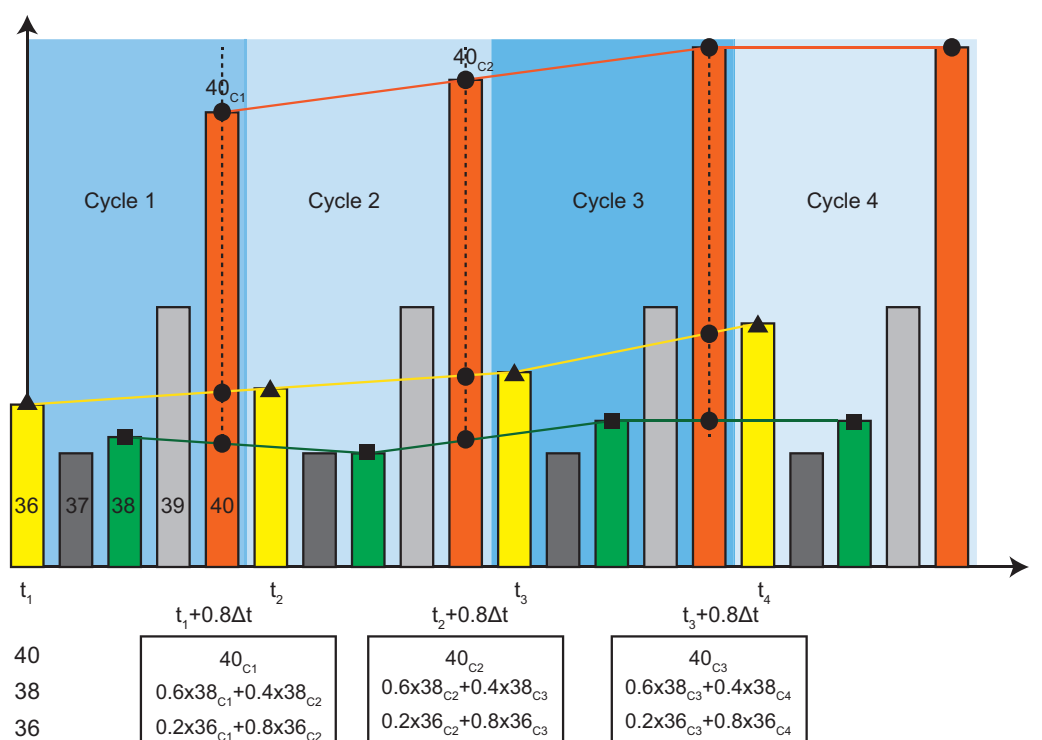


Figure 6.6 Schematic diagram of time interpolation used for correcting the differences in the timing of individual mass peak measurements. Because of the limited scan speed of a QMS, the timing of mass signal measurements differs for different mass numbers. To correct this effect, the isotopic ratios among ^{36}Ar , ^{38}Ar , and ^{40}Ar are calculated using the signal intensities of ^{36}Ar and ^{38}Ar corresponding to the timing when the QMS measures the ^{40}Ar signal.

C Sensitivity calibration of quadrupole mass spectrometer

The absolute sensitivity of QMS is essential to convert the QMS signal to the amount of ^{40}Ar . We performed calibration of QMS by introducing the known amount of air in the tank (Figure 6.7). The absolute amount of ^{40}Ar is calculated according to the readout of a Baratron manometer by

$$n_{atm} = \frac{pV}{RT} = \frac{p[\text{torr}]/760 \times 10.33 \times 10^{-3}}{0.082 \times 293} = 5.66 \times 10^{-7} p[\text{mol}]$$

$$n_{^{40}\text{Ar}} = 0.0093 n_{atm} = 5.26 \times 10^{-9} p[\text{mol}] = 1.18 \times 10^{-4} p[\text{cm}^3 \text{STP}]$$

Here we used the room temperature of our laboratory $T=293$ [K]. The example of calibration measurement is shown in Figure 6.8. The reproducibility of calibration coefficients during was $\sim 5\%$ (Figure 6.9).

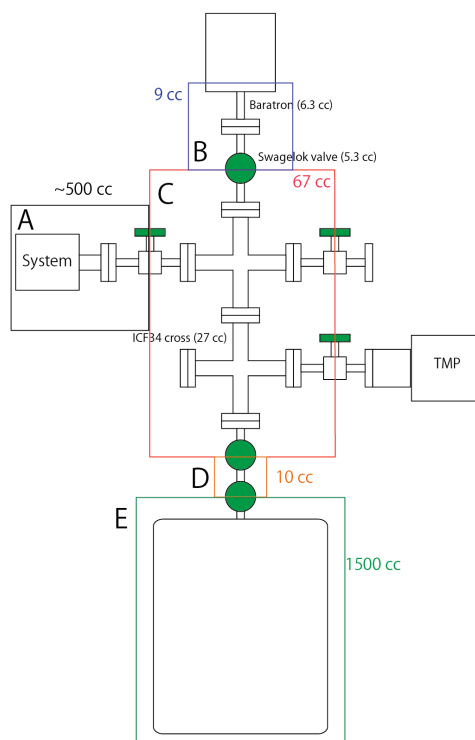


Figure 6.7 Schematic diagram of the calibration line. The calibration gas (diluted terrestrial atmosphere) is stored in the tank and the small portion of the gas is used in every calibration experiment.

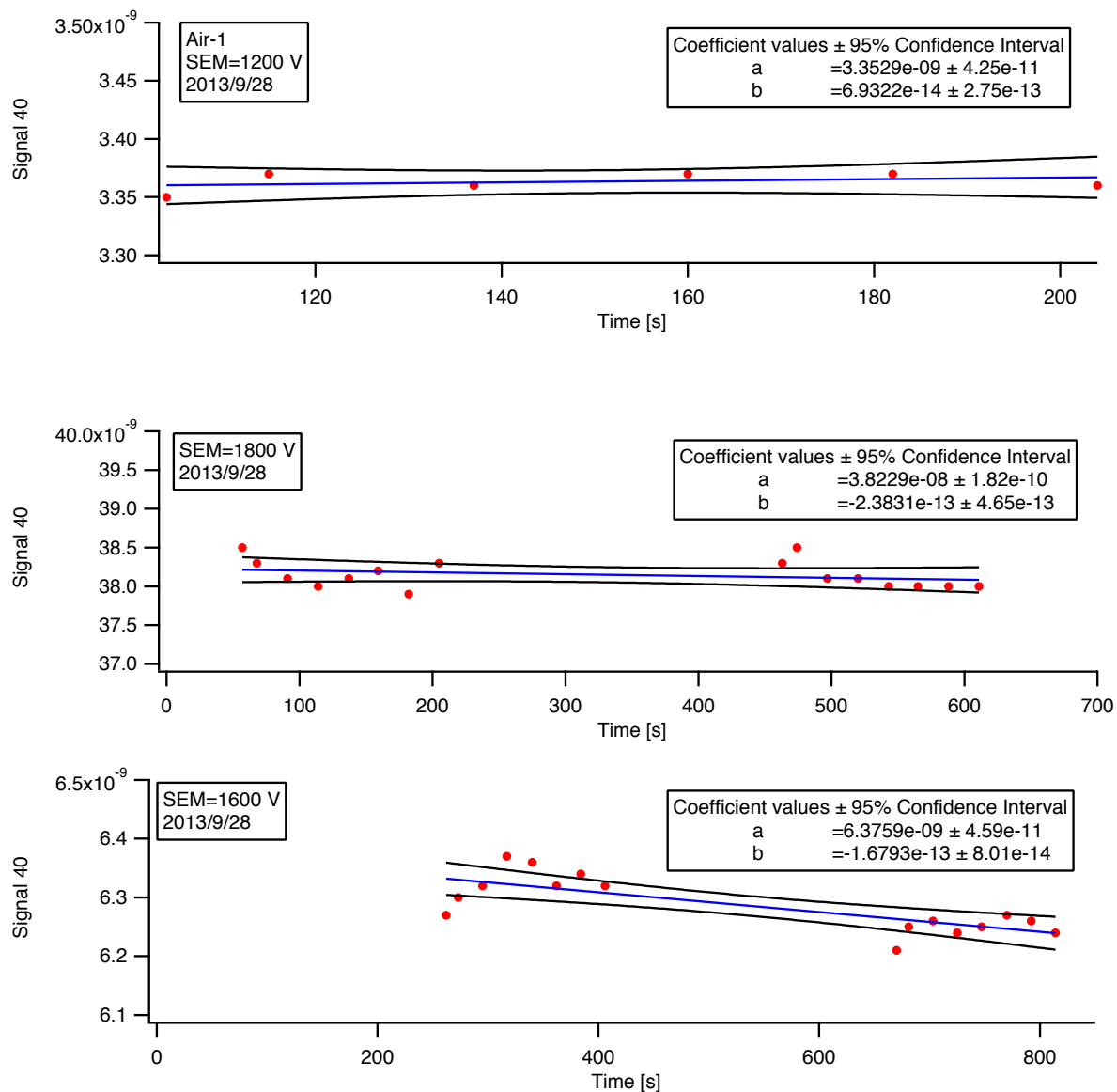


Figure 6.8 Time variation of QMS signals of ^{40}Ar with the different SEM voltages. Regression analyses are conducted to derive the amount of Ar gas at the time of gas introduction ($t=0$).

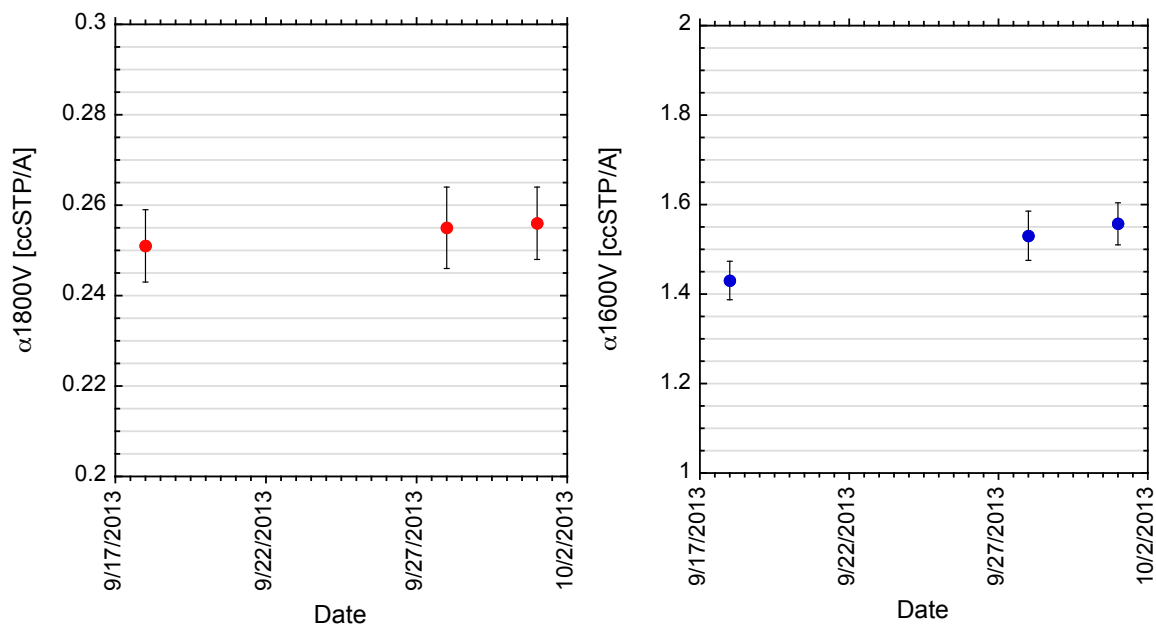


Figure 6.9 Sensitivity of the QMS system in terms of ⁴⁰Ar for different SEM voltages used in this study: (left) 1800V and (right) 1600V.

D Variation of blank level

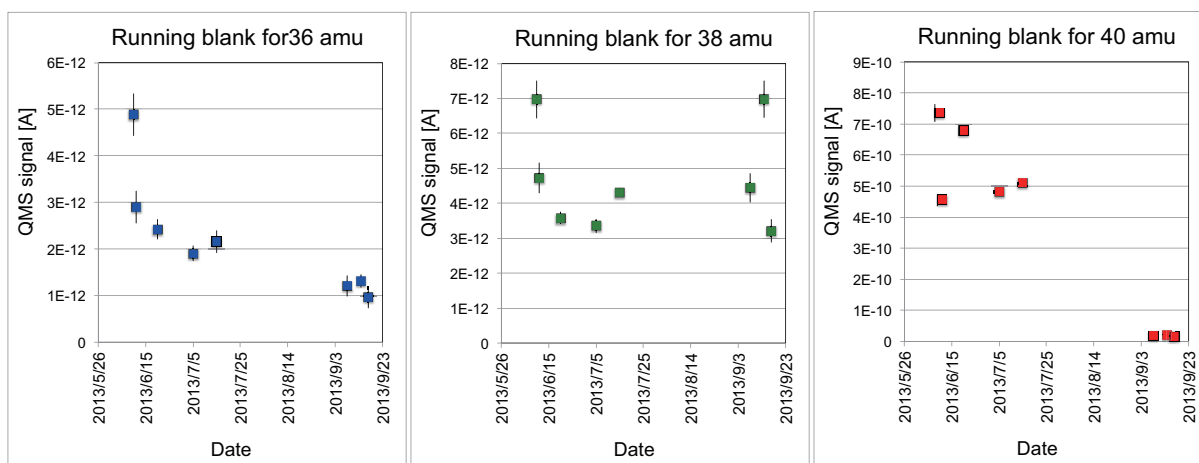


Figure 6.10 Stability of blank levels for the mass number of 36, 38, and 40. Note that the sample is replaced in early July, 2013.

E Elemental maps of gneiss samples

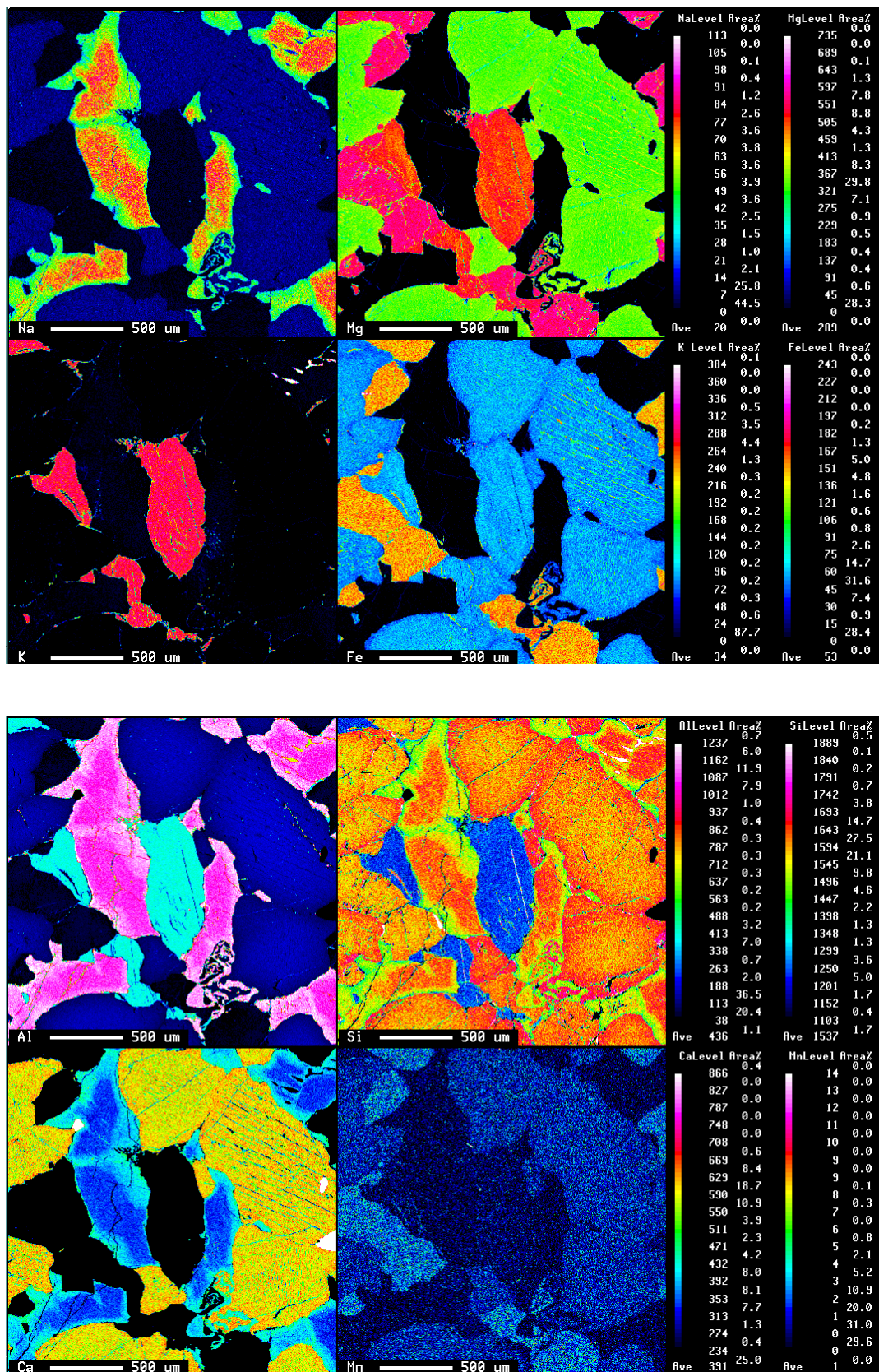


Figure 6.11 Elemental map of pyroxene-bearing gneiss.

References

- Acuña, M. H., et al. (1999), Global Distribution of Crustal Magnetization Discovered by the Mars Global Surveyor MAG/ER Experiment, *Science*, 284(5415), 790-793, doi:10.1126/science.284.5415.790.
- Aragón, C., and J. A. Aguilera (2008), Characterization of laser induced plasmas by optical emission spectroscopy: A review of experiments and methods, *Spectrochimica Acta Part B: Atomic Spectroscopy*, 63(9), 893-916, doi:10.1016/j.sab.2008.05.010.
- Barra, F., T. D. Swindle, R. L. Korotev, B. L. Jolliff, R. A. Zeigler, and E. Olson (2006), $^{40}\text{Ar}/^{39}\text{Ar}$ dating of Apollo 12 regolith: Implications for the age of Copernicus and the source of nonmare materials, *Geochimica et Cosmochimica Acta*, 70(24), 6016-6031, doi:10.1016/j.gca.2006.09.013.
- Bibring, J. P., et al. (2006), Global mineralogical and aqueous mars history derived from OMEGA/Mars Express data, *Science*, 312(5772), 400-404, doi:10.1126/science.1122659.
- Bogard, D. D. (2009), K-Ar dating of rocks on Mars: Requirements from Martian meteorite analyses and isochron modeling, *Meteorit. Planet. Sci.*, 44(1), 3-14.
- Bogard, D. D., and D. L. H. Garrison (1999), Argon-39-argon-40 "ages" and trapped argon in Martian shergottites, Chassigny, and Allan Hills 84001, *Meteorit. Planet. Sci.*, 34(3), 451-473.
- Bogard, D. D., L. Husain, and L. E. Nyquist (1978), ^{40}Ar - ^{39}Ar age of the Shergotty achondrite and implications for its post-shock thermal history, *Geochimica et Cosmochimica Acta*, 43, 1047-1055.
- Bogard, D. D., J. Park, and D. Garrison (2009), ^{39}Ar - ^{40}Ar "ages" and origin of excess ^{40}Ar in Martian shergottites, *Meteorit. Planet. Sci.*, 44, 905-923.
- Bottkejr, W., D. Durda, D. Nesvorny, R. Jedicke, A. Morbidelli, D. Vokrouhlicky, and H. Levison (2005), Linking the collisional history of the main asteroid belt to its dynamical excitation and depletion, *Icarus*, 179(1), 63-94, doi:10.1016/j.icarus.2005.05.017.

- Bouvier, A., J. Blichert-Toft, J. D. Vervoort, and F. Albarede (2005), The age of SNC meteorites and the antiquity of the Martian surface, *Earth Planet. Sci. Lett.*, *240*(2), 221-233, doi:10.1016/J.Epsi.2005.09.007.
- Boynton, W. V., et al. (2007), Concentration of H, Si, Cl, K, Fe, and Th in the low- and mid-latitude regions of Mars, *J. Geophys. Res.*, *112*(E12), doi:10.1029/2007je002887.
- Carr, M. (2006), *The Surface of Mars*, Cambridge University Press, New York.
- Carr, M. H. (1979), Formation of Martian flood features by release of water from confined aquifers, *J. Geophys. Res.*, *84*(B6), 2995, doi:10.1029/JB084iB06p02995.
- Carr, M. H., and J. W. Head (2010), Geologic history of Mars, *Earth Planet. Sci. Lett.*, *294*(3-4), 185-203, doi:10.1016/j.epsl.2009.06.042.
- Cho, Y., Y. N. Miura, and S. Sugita (2011), Development of a laser ablation isochron K-Ar dating method for landing planetary missions, *2011 PERC Planetary Geology Field Symposium Abstracts*, P30.
- Cho, Y., T. Morota, J. Haruyama, M. Yasui, N. Hirata, and S. Sugita (2012), Young mare volcanism in the Orientale region contemporary with the Procellarum KREEP Terrane (PKT) volcanism peak period ~2 billion years ago, *Geophys. Res. Lett.*, *39*(11), doi:10.1029/2012gl051838.
- Cho, Y., Y. N. Miura, and S. Sugita (2013), Development of an in-situ K-Ar isochron dating method using LIBS-QMS configuration, *Proc. Lunar Sci. Conf.*, *44*, 1505.
- Cintala, M. J., and R. A. F. Grieve (1998), Scaling impact melting and crater dimensions: Implications for the lunar cratering record, *Meteorit. Planet. Sci.*, *33*, 889-912.
- Clifford, S., and T. J. Parker (2001), The Evolution of the Martian Hydrosphere: Implications for the Fate of a Primordial Ocean and the Current State of the Northern Plains, *Icarus*, *154*(1), 40-79, doi:10.1006/icar.2001.6671.
- Cohen, B. A. (2012), Development of the potassium-argon laser experiment (KArLE) instrument for in-situ geochronology, *Proc. Lunar Sci. Conf.*, *43*, 1267.
- Corsi, M., G. Cristoforetti, M. Hidalgo, D. Iriarte, S. Legnaioli, V. Pelleschi, A. Salvetti, and E. Tognoni (2005), Effect of laser-induced crater depth in laser-induced breakdown spectroscopy emission features, *Applied Spectroscopy*, *59*, 853-860.

- Cousin, A., R. Wiens, V. Sautter, and N. Manfroid (2013), ChemCam analysis of Jake Matijevic, Gale crater, *Proc. Lunar Sci. Conf.*, 44, 1409.
- Deit, L. L., E. Hauber, F. Fueten, M. Pondrelli, A. P. Rossi, and R. Jaumann (2013), Sequence of infilling events in Gale Crater, Mars: Results from morphology, stratigraphy, and mineralogy, *Journal of Geophysical Research: Planets*, 118, 1-35, doi:10.1002/2012je004322.
- Devismes, D., P.-Y. Gillot, J.-C. Lefèvre, C. Boukari, E. Chassefière, and F. Chiavassa (2013), A K-Ar development based on UV laser for in situ geochronology on the surface of mars. Firsts results and isochrones, *EPSC abstracts*, 8, 71, doi:10.1126/science.1247166.
- Dickin, A. P. (2005), *Radiogenic Isotope Geology*, Second ed., Cambridge University Press, New York.
- Doran, P. T., et al. (2004), Mars chronology: assessing techniques for quantifying surficial processes, *Earth-Science Reviews*, 67(3-4), 313-337, doi:10.1016/j.earscirev.2004.04.001.
- Durda, D. D., R. Greenberg, and R. Jedicke (1998), Collisional Models and Scaling Laws: A New Interpretation of the Shape of the Main-Belt Asteroid Size Distribution, *Icarus*, 135, 431-440.
- Eugster, O., D. Terribilini, E. Polnau, and J. Kramers (2001), The antiquity indicator argon-40/argon-36 for lunar surface samples calibrated by uranium-235-xenon-136 dating, *Meteorit. Planet. Sci.*, 36, 1097-1115.
- Farley, K. A., et al. (2013), In Situ Radiometric and Exposure Age Dating of the Martian Surface, *Science express*, 1247166.
- Fassett, C. I., and J. W. Head (2008), The timing of martian valley network activity: Constraints from buffered crater counting, *Icarus*, 195(1), 61-89, doi:10.1016/j.icarus.2007.12.009.
- Gale, N. H., J. W. Arden, and R. Hutchison (1975), The chronology of the Nakhla achondritic meteorite, *Earth Planet. Sci. Lett.*, 26, 195-206.
- Ganapathy, R., and E. Anders (1969), Ages of calcium-rich achondrites-II, Howardites, nakhlites, and the Angra dos Reis angrite, *Geochimica et Cosmochimica Acta*, 33, 775-787.
- Geiss, J., and D. C. Hess (1958), Argon-potassium ages and the isotopic composition of argon from meteorites, *Astrophysical Journal*, 127, 224-236.

- Golombek, M., et al. (2012), Selection of the Mars Science Laboratory Landing Site, *Space Sci. Rev.*, 170(1-4), 641-737, doi:10.1007/s11214-012-9916-y.
- Greshake, A., J. Fritz, and D. Stöffler (2004), Petrology and shock metamorphism of the olivine-phyric shergottite Yamato 980459, *Geochimica et Cosmochimica Acta*, 68(10), 2359-2377, doi:10.1016/j.gca.2003.11.022.
- Grott, M., et al. (2012), Long-Term Evolution of the Martian Crust-Mantle System, *Space Sci. Rev.*, 174(1-4), 49-111, doi:10.1007/s11214-012-9948-3.
- Harris, R. D., D. A. Cremers, C. Khoo, and K. Benelli (2005), LIBS-BASED DETECTION OF GEOLOGICAL SAMPLES AT LOW PRESSURES (<0.0001 TORR) FOR MOON AND ASTEROID EXPLORATION, *Proc. Lunar Sci. Conf.*, 36, 1796.
- Hartman, W. K. (2003), Megaregolith evolution and cratering cataclysm models—Lunar cataclysm as a misconception (28 years later), *Meteorit. Planet. Sci.*, 38(4), 579-593.
- Hartman, W. K., M. Malin, A. McEwen, M. Carr, L. Soderblom, P. Thomas, E. Danielson, P. James, and J. Veverka (1999), Evidence for recent volcanism on Mars from crater counts, *Nature*, 397, 586-589.
- Hartmann, W. K. (2005), Martian cratering 8: Isochron refinement and the chronology of Mars, *Icarus*, 174(2), 294-320, doi:10.1016/j.icarus.2004.11.023.
- Hartmann, W. K., and G. Neukum (2001), Cratering chronology and the evolution of Mars, *Space Sci. Rev.*, 96, 165-194, doi:10.1023/A:1011989004263.
- Hartmann, W. K., C. Quantin, and N. Mangold (2007), Possible long-term decline in impact rates, *Icarus*, 186(1), 11-23, doi:10.1016/j.icarus.2006.09.009.
- Haruyama, J., et al. (2009), Long-lived volcanism on the lunar farside revealed by SELENE Terrain Camera, *Science*, 323, 905-908, doi:10.1126/science.1163382.
- Haskin, L. A., R. L. Korotev, K. M. Rockow, and B. L. Jolliff (1998), The case for an Imbrium origin of the Apollo thorium-rich impact-melt breccias, *Meteorit. Planet. Sci.*, 33(5), 959-975.
- Hiesinger, H., J. W. Head, U. Wolf, R. Jaumann, and G. Neukum (2003), Ages and stratigraphy of mare basalts in Oceanus Procellarum, Mare Nubium, Mare Cognitum, and Mare Insularum, *J. Geophys. Res.*, 108(E7), 5065, doi:10.1029/2002je001985.

- Hohenberg, C. M., K. Marti, F. A. Podosek, R. C. Reedy, and J. R. Shirck (1978), Comparison between observed and predicted cosmogenic noble gases in lunar samples, *Proc. Lunar Sci. Conf., IX*, 2311-2344.
- Hollister, L. S., and M. L. Crawford (1977), Melt immiscibility in Apollo 15 KREEP: Origin of Fe-rich mare basalts, *Proc. Lunar Sci. Conf., 8*, 2419-2432.
- Humayun, M., and R. N. Clayton (1995), Potassium Isotope Cosmochemistry - Genetic Implications of Volatile Element Depletion, *Geochimica Et Cosmochimica Acta*, 59(10), 2131-2148, doi:10.1016/0016-7037(95)00132-8.
- Ivanov, B. A. (2001), Mars/Moon cratering rate ratio estimates, *Space Science Review*, 96, 87-104.
- Iwata, N. (2003), K-Ar ages of the Massifs A, B, C and the Minami-Yamato Nunataks, Yamato Mountains, East Antarctica, *Goldschmidt Conference Abstracts*, A182.
- Iwata, N. (2007), K-Ar ages of gneisses from the Mt. Riiser-Larsen area, Naper Complex, East Antarctica, paper presented at 27th Symposium on Polar Geosciences.
- Jolliff, B. L., J. Gillis, L. A. Haskin, R. L. Korotev, and M. A. Wieczorek (2000), Major lunar crustal terranes: Surface expressions and crust-mantle origins, *J. Geophys. Res.*, 105(E2), 4197-4216, doi:10.1029/1999JE001103.
- Kelley, S. (2002), K-Ar and Ar-Ar Dating, *Reviews in Mineralogy and Geochemistry*, 47(1), 785-818, doi:10.2138/rmg.2002.47.17.
- Knight, A. K., N. L. Scherbarth, D. A. Cremers, and M. J. Ferris (2000), Characterization of laser-induced breakdown spectroscopy (LIBS) for application to space exploration, *Applied Spectroscopy*, 54(3), 331-340, doi: 10.1366/0003702001949591.
- Kobayashi, H., and H. Tanaka (2010), Fragmentation model dependence of collision cascades, *Icarus*, 206(2), 735-746, doi:10.1016/j.icarus.2009.10.004.
- Kobayashi, S., et al. (2010), Determining the Absolute Abundances of Natural Radioactive Elements on the Lunar Surface by the Kaguya Gamma-ray Spectrometer, *Space Sci. Rev.*, 154(1-4), 193-218, doi:10.1007/s11214-010-9650-2.
- Lapen, T. J., M. Richter, A. D. Brandon, V. Debaille, B. L. Beard, J. T. Shafer, and A. H. Peslier (2010), A younger age for ALH84001 and its geochemical link to shergottite sources in Mars, *Science*, 328(5976), 347-351, doi:10.1126/science.1185395.

- Lasue, J., R. C. Wiens, S. M. Clegg, D. T. Vaniman, K. H. Joy, S. Humphries, A. Mezzacappa, N. Melikechi, R. E. McInroy, and S. Bender (2012), Remote laser-induced breakdown spectroscopy (LIBS) for lunar exploration, *J. Geophys. Res.*, *117*(E01002), doi:10.1029/2011je003898.
- Lawrence, D. J. (1998), Global Elemental Maps of the Moon: The Lunar Prospector Gamma-Ray Spectrometer, *Science*, *281*(5382), 1484-1489, doi:10.1126/science.281.5382.1484.
- Lawrence, D. J., R. C. Puetter, R. C. Elphic, W. C. Feldman, J. J. Hagerty, T. H. Prettyman, and P. D. Spudis (2007), Global spatial deconvolution of Lunar Prospector Th abundances, *Geophys. Res. Lett.*, *34*(3), doi:10.1029/2006gl028530.
- Loddoch, A., and U. Hansen (2008), Temporally transitional mantle convection: Implications for Mars, *J. Geophys. Res.*, *113*(E9), doi:10.1029/2007je003023.
- Ludwig, K. R. (2009), Isoplot4.15, edited, Berkeley Geochronology Center.
- Lugmair, G. W., and C. W. Carlson (1978), The Sm-Nd history of KREEP, *Proc. Lunar Sci. Conf.*, *IX*, 689-704.
- Mahaffy, P. R., et al. (2012), The Sample Analysis at Mars Investigation and Instrument Suite, *Space Sci. Rev.*, *170*(1-4), 401-478, doi:10.1007/s11214-012-9879-z.
- Marchi, S., et al. (2013), High-velocity collisions from the lunar cataclysm recorded in asteroidal meteorites, *Nature Geoscience*, *6*(4), 303-307, doi:10.1038/ngeo1769.
- Maurice, S., et al. (2012), The ChemCam Instrument Suite on the Mars Science Laboratory (MSL) Rover: Science Objectives and Mast Unit Description, *Space Sci. Rev.*, *170*(1-4), 95-166, doi:10.1007/s11214-012-9912-2.
- Melosh, H. J. (1989), *Impact Cratering -A Geologic Process-*, Oxford University Press, New York.
- Mermet, J. M. (2008), Limit of quantitation in atomic spectrometry: An unambiguous concept?, *Spectrochimica Acta Part B: Atomic Spectroscopy*, *63*(2), 166-182, doi:10.1016/j.sab.2007.11.029.
- Mermet, J. M. (2010), Calibration in atomic spectrometry: A tutorial review dealing with quality criteria, weighting procedures and possible curvatures, *Spectrochimica Acta Part B-Atomic Spectroscopy*, *65*(7), 509-523, doi: 10.1016/J.Sab.2010.05.007.
- Meyer, C. (2003), Shergotty, *Mars Meteorite Compendium 2003*.

- Meyer, C. (2004a), 15382 KREEP Basalt, *Lunar Sample Compendium*.
- Meyer, C. (2004b), 15386 KREEP Basalt, *Lunar Sample Compendium*.
- Meyer, C. (2012), Zagami, *Martian Meteorite Compendium*.
- Milam, K. A., K. R. Stockstill, J. E. Moersch, Harry Y. McSween Jr., L. L. Tornabene, and A. Ghosh (2003), THEMIS characterization of the MER Gusev crater landing site, *J. Geophys. Res.*, *108*(E12), 8078, doi:10.1029/2002je002023.
- Ming, D. W., et al. (2008), Geochemical properties of rocks and soils in Gusev Crater, Mars: Results of the Alpha Particle X-Ray Spectrometer from Cumberland Ridge to Home Plate, *J. Geophys. Res.*, *113*, E12S39, doi:10.1029/2008je003195.
- Minitti, M. E., et al. (2013), Mars Hand Lems Imager (MAHLI) observations of rocks at Curiosity's field site, Sols 0-100, *Proc. Lunar Sci. Conf.*, *44*, 2186.
- Miura, Y. N., K. Nagao, N. Sugiura, H. Sagawa, and K. Matsubara (1995), Orthopyroxenite ALH84001 and shergottite ALH77005: Additional evidence for a martian origin from noble gases, *Geochimica et Cosmochimica Acta*, *59*(10), 2105-2113.
- Morota, T., et al. (2011), Timing and characteristics of the latest mare eruption on the Moon, *Earth Planet. Sci. Lett.*, *302*, 255-266, doi:10.1016/j.epsl.2010.12.028.
- Neukum, G. (1983), Meteoritenbombardement und Datierung planetarer Oberflächen, Ludwig-Maximilians-University, Munich, Germany.
- Neukum, G., A. T. Basilevsky, T. Kneissl, M. G. Chapman, S. van Gasselt, G. Michael, R. Jaumann, H. Hoffmann, and J. K. Lanz (2010), The geologic evolution of Mars: Episodicity of resurfacing events and ages from cratering analysis of image data and correlation with radiometric ages of Martian meteorites, *Earth Planet. Sci. Lett.*, *294*(3-4), 204-222, doi:10.1016/j.epsl.2009.09.006.
- Neukum, G., et al. (2004), Recent and episodic volcanic and glacial activity on Mars revealed by the High Resolution Stereo Camera, *Nature*, *432*, 971-979.
- Ng, C. W., W. F. Ho, and N. H. Cheung (1997), Spectrochemical analysis of liquids using laser-induced plasma emissions: Effects of laser wavelength on plasma properties, *Applied Spectroscopy*, *51*(7), 976-983, doi:10.1366/0003702971941638.
- Nimmo, F., and K. Tanaka (2005), Early Crustal Evolution of Mars, *Annual Review of Earth and*

- Planetary Sciences*, 33(1), 133-161, doi:10.1146/annurev.earth.33.092203.122637.
- Norman, M. D., R. A. Duncan, and J. J. Huard (2006), Identifying impact events within the lunar cataclysm from ^{40}Ar – ^{39}Ar ages and compositions of Apollo 16 impact melt rocks, *Geochimica et Cosmochimica Acta*, 70(24), 6032-6049, doi:10.1016/j.gca.2006.05.021.
- Nyquist, L. E., B. M. Bansal, and H. Wiesmann (1975), Rb-Sr ages and initial $^{87}\text{Sr}/^{86}\text{Sr}$ for Apollo 17 basalts and KREEP basalt 15386, *Proc. Lunar Sci. Conf.*, 6, 610-612.
- Nyquist, L. E., C.-Y. Shih, D. D. Bogard, and A. Yamaguchi (2010a), Lunar crustal history from isotopic studies of lunar anorthosites, *GLUC-2010*.
- Nyquist, L. E., C.-Y. Shih, and Y. D. Reese (2010b), Rb-Sr and Sm-Nd ages of Zagami DML and Sr isotopic heterogeneity in Zagami, *73rd Annual Meteoritical Society Meeting*, 5243.
- Nyquist, L. E., J. Wooden, B. Bansal, H. Wiesmann, G. McKay, and D. D. Bogard (1979), Rb-Sr age of the Shergotty achondrite and implications for metamorphic resetting of isochron ages, *Geochimica et Cosmochimica Acta*, 43(1057-1074).
- Ozima, M., Y. N. Miura, and F. A. Podosek (2004), Orphan radiogenic noble gases in lunar breccias: evidence for planet pollution of the Sun?, *Icarus*, 170(1), 17-23, doi:10.1016/j.icarus.2004.02.007.
- Ozima, M., K. Seki, N. Terada, Y. N. Miura, F. A. Podosek, and H. Shinagawa (2005), Terrestrial nitrogen and noble gases in lunar soils, *Nature*, 436(7051), 655-659, doi:10.1038/nature03929.
- Papike, J. J., G. W. Fowler, and C. K. Shearer (1997), Evolution of the lunar crust: SIMS study of plagioclase from ferroan anorthosites, *Geochimica et Cosmochimica Acta*, 61(11), 2343-2350.
- Phillips, R. J., et al. (2001), Ancient geodynamics and global-scale hydrology on Mars, *Science*, 291(5513), 2587-2591, doi:10.1126/science.1058701.
- Robbins, S. J., G. D. Achille, and B. M. Hynek (2011), The volcanic history of Mars: High-resolution crater-based studies of the calderas of 20 volcanoes, *Icarus*, 211(2), 1179-1203, doi:10.1016/j.icarus.2010.11.012.
- Russo, R. E., X. Mao, H. Liu, J. Gonzalez, and S. S. Mao (2002), Laser ablation in analytical chemistry—a review, *Talanta*, 57, 425-451.

- Sallé, B., J. L. Lacour, P. Mauchien, P. Fichet, S. Maurice, and G. Manhès (2006), Comparative study of different methodologies for quantitative rock analysis by Laser-Induced Breakdown Spectroscopy in a simulated Martian atmosphere, *Spectrochimica Acta Part B: Atomic Spectroscopy*, *61*(3), 301-313, doi:10.1016/j.sab.2006.02.003.
- Schmidt, M. E., et al. (2013), APXS of first rocks encountered by Curiosity in Gale crater: geochemical diversity and volatile element (K and Zn) enrichment, *Proc. Lunar Sci. Conf.*, *44*, 1278.
- Shannon, M. A. (1998), A simplified cavity analysis for estimating energy coupling during laser ablation and drilling of solids - theory, *Applied Surface Science*, *127*, 218-225, doi:10.1016/S0169-4332(97)00635-1.
- Shervais, J. W., L. A. Taylor, J. C. Laul, C.-Y. Shih, and L. E. Nyquist (1985), Very high potassium (VHK) basalt: complications in mare basalt petrogenesis, *J. Geophys. Res.*, *90*, D3-D18.
- Spohn, T., W. Konrad, D. Breuer, and R. Ziethe (2001), The Longevity of Lunar Volcanism: Implications of Thermal Evolution Calculations with 2D and 3D Mantle Convection Models, *Icarus*, *149*(1), 54-65, doi:10.1006/icar.2000.6514.
- Steiger, R. H., and E. Jäger (1977), Subcommission on geochronology: convention on the use of decay constants in geo- and cosmochemistry, *Earth Planet. Sci. Lett.*, *36*, 359-362.
- Stephen, N. R., G. K. Benedix, P. A. Bland, K. T. Howard, and V. E. Hamilton (2010), Modal mineralogy of the Martian meteorite Zagami, *Proc. Lunar Sci. Conf.*, *XLI*(2367).
- Stettler, A., P. Eberhardt, J. Geiss, N. Großgler, and P. Maurer (1973), ³⁹Ar–⁴⁰Ar ages and ³⁷Ar–³⁸Ar exposure ages of lunar rocks, *Proc. Lunar Sci. Conf.*, *4*, 1865–1888.
- Stipe, C. B., E. Guevara, J. Brown, and G. R. Rossman (2012), Quantitative laser-induced breakdown spectroscopy of potassium for in-situ geochronology on Mars, *Spectrochimica Acta Part B-Atomic Spectroscopy*, *70*, 45-50, doi:10.1016/J.Sab.2012.04.010.
- Stöffler, D., and G. Ryder (2001), Stratigraphy and isotope ages of lunar geologic units: chronological standard for the inner solar system, *Space Sci. Rev.*, *96*, 9-54.
- Stolper, E., and H. Y. McSween (1979), Petrology and origin of the shergottite meteorites, *Geochimica et Cosmochimica Acta*, *43*, 1475-1498.
- Stolper, E. M., et al. (2013), The petrochemistry of Jake_M: a martian mugearite, *Science*,

- 341(6153), 1239463, doi:10.1126/science.1239463.
- Swindle, T. D. (2001), Could in-situ dating work on Mars?, *Proc. Lunar Sci. Conf.*, XXXII(1492).
- Swindle, T. D., R. Bode, W. V. Boynton, D. A. Kring, M. Williams, A. Chutjian, M. R. Darrach, D. A. Cremers, R. C. Wiens, and S. L. Baldwin (2003), AGE (Argon Geochronology Experiment): an instrument for in situ geochronology on the surface of Mars, *Proc. Lunar Sci. Conf.*, XXXIV, Abstract #1488.
- Swindle, T. D., and E. K. Olson (2004), ⁴⁰Ar-³⁹Ar studies of whole rock nakhlites: Evidence for the timing of formation and aqueous alteration on Mars, *Meteorit. Planet. Sci.*, 39(5), 755-766.
- Takeda, H., M. Miyamoto, M. B. Duke, and T. Ishii (1978), Crystallization of pyroxenes in lunar KREEP basalt 15386 and meteoritic basalts, *Proc. Lunar Sci. Conf.*, 9, 1157-1171.
- Takeda, H., and H. Mori (1984), Mesostasis-rich lunar and eucritic basalts with reference to REE-rich minerals, *Proc. Lunar Sci. Conf.*
- Talboys, D. L., et al. (2009), In situ radiometric dating on Mars: Investigation of the feasibility of K-Ar dating using flight-type mass and X-ray spectrometers, *Planet. Space Sci.*, 57(11), 1237-1245, doi:10.1016/j.pss.2009.02.012.
- Tanaka, K. L. (1986), The Stratigraphy of Mars, *Journal of Geophysical Research-Solid Earth and Planets*, 91(B13), E139-E158, doi:10.1029/Jb091ib13p0e139.
- Tera, F., Papanast.Da, and Wasserbu.Gj (1974), Isotopic Evidence for a Terminal Lunar Cataclysm, *Earth Planet. Sci. Lett.*, 22(1), 1-21, doi:10.1016/0012-821x(74)90059-4.
- Treiman, A. H. (2005), The nakhlite meteorites: Augite-rich igneous rocks from Mars, *Chemie der Erde - Geochemistry*, 65(3), 203-270, doi:10.1016/j.chemer.2005.01.004.
- Tsiganis, K., R. Gomes, A. Morbidelli, and H. F. Levison (2005), Origin of the orbital architecture of the giant planets of the Solar System, *Nature*, 435(7041), 459-461, doi:10.1038/nature03539.
- Vaucher, J., D. Baratoux, N. Mangold, P. Pinet, K. Kurita, and M. Grégoire (2009), The volcanic history of central Elysium Planitia: Implications for martian magmatism, *Icarus*, 204(2), 418-442, doi:10.1016/j.icarus.2009.06.032.
- Wieczorek, M. A., and R. J. Phillips (2000), The "Procellarum KREEP Terrane": Implications for

- mare volcanism and lunar evolution, *J. Geophys. Res.*, 105(E8), 20417-20430, doi:10.1029/1999JE001092.
- Wright, I. P., M. R. Sims, and C. T. Pillinger (2000), Scientific objectives of the Beagle 2 lander, *Acta Astronautica*, 52, 219-225.
- Wyatt, M. B., H. Y. McSween, K. L. Tanaka, and J. W. Head (2004), Global geologic context for rock types and surface alteration on Mars, *Geology*, 32(8), 645, doi:10.1130/g20527.1.
- York, D. (1969), Least squares fitting of a straight line with correlated errors, *Earth Planet. Sci. Lett.*, 5, 320-324.
- Ziethé, R., K. Seiferlin, and H. Hiesinger (2009), Duration and extent of lunar volcanism: Comparison of 3D convection models to mare basalt ages, *Planet. Space Sci.*, 57(7), 784-796, doi:10.1016/j.pss.2009.02.002.